Arch Biol Sci. 2024;76(4):431-444 https://doi.org/10.2298/ABS240720033F

Involvement of the TGF-β pathway in epithelial-mesenchymal transition promoted by the pulmonary microenvironment in *Mycoplasma pneumoniae* pneumonia

Lu Fan[1], Huixia Wang[2], Nuo Xu[3], Yun Guo[1,3,*] and Ling Li[1,3,#]

[1]*Department of Respiratory Medicine and Clinical Allergy Center, The Affiliated Children's Hospital of Jiangnan University*, Wuxi, 214000, China

[2]*Department of Pediatric Respiratory Medicine, Pediatric Respiratory Medicine of Zhumadian Central Hospital*, Zhumadian, 463000, China

[3]*Department of Respiratory Medicine and Clinical Allergy Center, The Affiliated Wuxi Peoples' Hospital of Nanjing Medical University, Wuxi Children's Hospital*, Wuxi, 214000, China

Corresponding authors: *guoyun@jiangnan.edu.cn; #liling@njmu.edu.cn

Received: July 20, 2024; **Revised**: September 5, 2024; **Accepted**: October 1, 2024; **Published online**: October 28, 2024

Abstract: Abstract: *Mycoplasma pneumoniae* (MP), one of the smallest prokaryotic microorganisms capable of independent survival, causes respiratory tract infections and various extrapulmonary diseases. *Mycoplasma pneumoniae* pneumonia (MPP) is the most significant clinical manifestation, often leading to complications such as atelectasis and pulmonary fibrosis. We explored the role of the pulmonary microenvironment in regulating epithelial-mesenchymal transition (EMT) in MPP patients with atelectasis. Transcriptome sequencing revealed significant upregulation of pathways including transforming growth factor beta (TGF-β), tumor protein 53 (P53), protein kinase Hippo, Ras-proximate-1 or Ras-related protein 1 (Rap1), and members of class O forkhead box proteins (FoxO) in cells exposed to bronchoalveolar lavage fluid (BALF) from MPP patients with atelectasis. Among these, the TGF-β pathway exhibited the most pronounced changes in gene expression. Further analysis confirmed that BALF from these patients induced EMT in human bronchial epithelial cells and mouse lung tissues and that TGF-β receptor kinase inhibitor (TRKI) effectively reversed this process. In conclusion, the pulmonary microenvironment in MPP patients with atelectasis promotes EMT in the lungs, with TGF-β playing a key role in this process. This may represent a crucial mechanism contributing to pulmonary fibrosis, underscoring the need to focus on the pulmonary microenvironment and TGF-β-targeted therapies for the prevention and management of pulmonary fibrosis in these patients.

Keywords: *Mycoplasma pneumoniae* pneumonia (MPP); atelectasis; microenvironment; epithelial-mesenchymal transition (EMT); TGF-β

INTRODUCTION

Mycoplasma pneumoniae (MP), the smallest free-living prokaryote, has a unique capacity for *in vitro* growth under cell-free conditions. MP infection is a widespread phenomenon accounting for about 37% of community-acquired pneumonia cases [1, 2]. MP infection can lead to *Mycoplasma pneumoniae* pneumonia (MPP), which affects the respiratory tract and is associated with various extrapulmonary complications, such as meningoencephalitis, myocarditis, and atherosclerosis [3-5]. With increasing drug resistance, some patients may progress to severe pneumonia and/or refractory MPP with pleural effusion fluid, multiple organ dysfunction, and severe long-term complications [6].

As the disease progresses, it can lead to mucus plug formation and impaired ventilation function, which contribute to alveolar collapse, and atelectasis [6, 7]. This obstruction impedes the expulsion of necrotic epithelial cells and inflammatory secretions, potentially leading to further complications such as lung abscesses and organizing pneumonia [8]. Even in severe cases, pneumonectomy may be necessary as an intervention [9, 10]. As the disease progresses, some patients with MPP-related atelectasis, although pulmonary obstruction is relieved, continue to develop pulmonary complications, most commonly pulmonary fibrosis. Our study focused on exploring the critical role of the MPP-altered lung tissue environment in promoting these complications.

Epithelial-mesenchymal transition (EMT) exacerbates fibrosis by generating fibroblasts and myofibroblasts that secrete collagen and other extracellular matrix (ECM) proteins, leading to tissue sclerosis and loss of function [11, 12]. During EMT, epithelial cells lose their polarity and adhesion properties, acquiring mesenchymal traits that increase their invasive and migratory capacities [13]. This cellular transformation, which is pivotal in the development of pulmonary fibrosis, is typically marked by the downregulation of E-cadherin and upregulation of mesenchymal markers such as fibronectin, vimentin, and alpha smooth muscle actin (αSMA) [14]. The process of EMT involves the loss of epithelial markers and the acquisition of mesenchymal markers, enabling cancer cells to migrate and invade distant tissues [15].

EMT plays a role in the damage and repair of lung inflammation, while MP contributes to lung inflammation through mechanisms such as adhesion, virulence factors, and the immune response [16-19]. Studies have shown that MP infection can induce the occurrence of EMT in the lungs of mice [20]. However, the relationship between the pulmonary microenvironment in MPP patients and the phenomenon of EMT remains unclear.

This study aimed to elucidate the relationship between the altered pulmonary microenvironment in MPP patients with atelectasis and EMT through both *in vivo* and *in vitro* experiments. We demonstrate how this process may contribute to the chronicity of the disease in these patients.

MATERIALS AND METHODS

Ethics statement

All experiments were conducted following the directions of the NIH (National Research Council) Guide for the Care and Use of Laboratory Animals. Experimental animals were provided by the Jiangsu Human Organ Transplantation Center Laboratory. The animal experiments were approved by the ethics review of Wuxi Clinical Medical College Affiliated with Nanjing Medical University. Ethical approval for the study involving human subjects was obtained from the Ethics Committee of Wuxi Children's Hospital (Ethics Approval No. WXCH2020-03-003). The privacy rights of human subjects were observed and informed consent was obtained for experimentation with human subjects. The research was conducted per the principles of the Declaration of Helsinki and in compliance with local regulatory requirements.

BALF samples from MPP patients

A total of 120 MPP patients were included in this study, from whom 38 bronchoalveolar lavage fluid (BALF) and 120 sputum samples collected. Patient characteristics and basic clinical information were recorded (Supplementary Table S1). The BALF samples were collected from patients who met the enrollment requirements in the Respiratory Department of Wuxi Children's Hospital from January to December 2020. The inclusion criteria for MPP patients without atelectasis were as follows: (i) clinical manifestations that met the diagnostic criteria for pneumonia; (ii) peripheral blood culture or sputum culture revealing the presence of the MP-IgM antibody; the titer was ≥1:160. Exclusion criteria were: (i) laboratory tests that showed positive results for other pathogens; (ii) other systemic diseases, such as those involving the cardiovascular system, nervous system, and blood system present on admission; (iii) diseases of the respiratory system present on admission, such as bronchial asthma, obliterative bronchiolitis, congenital bronchopulmonary dysplasia, etc. An additional inclusion criterion for MPP patients with atelectasis was a chest X-ray or computed tomography (CT) showing atelectasis on one side of the lung. BALF samples were collected from 35 MPP patients with atelectasis and 3 MPP patients without atelectasis. The BALF was initially filtered to eliminate thick liquids such as sputum. It was then sterilized using ultraviolet light for 30 min to 1 h. Equal quantities of sterilized BALF were put into 1.5 mL Eppendorf Tubes, stored in a -80°C freezer, and mixed before use.

Cell culture

BEAS-2B epithelial cells isolated from normal human bronchial epithelium derived from autopsies of non-cancerous individuals and adenocarcinomic human alveolar basal epithelial A549 cells were cultured in Dulbecco's modified Eagle's medium (DMEM) (US

Biological, USA) supplemented with 10% fetal bovine serum (Gibco, USA), and 2% penicillin/streptomycin (HyClone, USA). The cells were grown in a humidified atmosphere comprising 95% air and 5% CO_2 at 37°C.

Cell scratch assay

About 5×10^5 cells were seeded in 6-well plates with 2 mL of DMEM per well. Final concentrations of 10% BALF and 10 μmol/L TGF-β receptor kinase inhibitor (TRKI, a selective inhibitor of TGF-β Type I receptor/ALK5, ALK4, ALK7) (MCE, USA) were added, and the same volume of phosphate-buffered saline (PBS) was added to a 6-well plate as a blank control. The 6-well plates were placed in a cell culture incubator at a constant temperature of 37°C and photographed under a white light microscope at 24 h of culture; the scratch images were analyzed using ImageJ software. The calculation formula for the migration rate was as follows:

$$\text{migration rate} = [1-(S24\ h/S0\ h)]\times100\%$$

Experiments were performed in triplicate and repeated 3 times.

Immunofluorescence staining

Cells were cultured for 24 h, followed by treatment with PBS, BALF, or BALF combined with TRKI for 72 h. After removal of the supernatant, the cells were fixed with 4% paraformaldehyde for 20 min, washed with PBS, and permeabilized with 0.3% Triton for 10 min. Blocking was performed with 0.3% Triton containing 10% goat serum for 1 h at 37°C. Primary antibodies, E-cadherin Rabbit mAb (Cell Signaling Technology, USA) and anti-alpha smooth muscle actin antibody (Abcam, UK) were diluted in 10% goat serum with 0.3% Triton, 50 μL were added per well, and incubated overnight at 4°C. After washing with PBS, 50 μL per well of secondary antibodies Alexa Fluor 488 anti-rabbit IgG (Invitrogen, USA) and Alexa Fluor 594 anti-mouse IgG (Invitrogen, USA) were added, incubated at 37°C in the dark for 1 h, and then washed. The cells were stained with 4',6-diamidino-2-phenylindole (DAPI) (Invitrogen, USA), washed, and finally, the slides were sealed with an anti-fluorescence quencher. Images were then taken using an SP8 Fluorescence Confocal Microscope.

Western blotting

Total proteins were extracted using radioimmunoprecipitation assay (RIPA) buffer. Total proteins were then separated by 10% sodium dodecyl sulfate-polyacrylamide gel electrophoresis (SDS-PAGE) and transferred to a nitrocellulose (NC) membrane. After incubation with the primary and secondary antibodies, the immunoreactive bands were detected with enhanced chemiluminescence (ECL) reagent.

Enzyme-linked immunosorbent assay (ELISA)

The sputum from MPP patients was divided into an atelectasis group and a non-atelectasis group. Sputum was diluted at a 1:1 ratio, and the supernatant was collected. The expression of TGF-β1 was detected using the human TGF-β1 Quantikine ELISA kit (R&D Systems, USA).

Animal model

Nine healthy adult C57BL/6 laboratory mice, meticulously nurtured in a strictly controlled specific pathogen-free (SPF) animal facility, were uniformly divided into 3 distinct groups: the PBS group, the BALF intervention group and the BALF combined with TRKI intervention group. The mice were anesthetized with 1% pentobarbital sodium solution at 50 mg/kg. Using a sterile insulin syringe, the BALF group received an intratracheal injection of 10 μL of BALF. Immediately after injection, the mouse's head was tilted upward at a 45° angle for 30 s, and deep breathing was observed. The neck incision was then aseptically sutured. The PBS group received an intratracheal injection of 10 μL of PBS. The BALF combined with TRKI group received an intratracheal injection of 10 μL of BALF, and an intraperitoneal injection of 100 μL of 1 μmol/L TRKI for 3 consecutive days. On the 4th day, the nine mice were killed, and the lung tissue was quickly harvested, placed in liquid nitrogen, and then stored at -80°C or fixed in paraformaldehyde for subsequent experiments.

Hematoxylin and eosin (H&E) staining

After lavage, lung tissues were fixed with 4% paraformaldehyde at room temperature. Paraffin-embedded mouse lung tissue was sliced into 5-μm sections using a

microtome. The sections were carefully placed on glass slides coated with polylysine and dried in an oven at 60°C for 4 h. The sections were first soaked in xylene for 30 min, followed by a second soak in clean xylene for 10 min to complete the dewaxing process, followed by gradient alcohol rehydration using an automatic program, and staining with 0.5% eosin for 2 min. Dehydration and transparency processes were initiated using a low concentration of alcohol. The sections were then observed and photographed under a microscope.

RNA sequencing analysis

BALF samples were collected from 6 patients: 3 were diagnosed with MPP accompanied by atelectasis, while the remaining 3 were diagnosed with MPP without atelectasis. Each BALF group was used to treat 3 independent cell cultures, resulting in a total of 3 biological replicates for each group. RNA was extracted from these samples for comprehensive transcriptomic analysis. Total RNA was isolated and extracted from cells using the EZ-press RNA Purification Kit (EZBioscience, USA) according to the manufacturer's instructions. The NEBNext® Ultra™ RNA Library Prep Kit for Illumina® (NEB, USA) was then used to generate ANA sequencing libraries. Sequencing was conducted by Annoroad (China), with the primed 150-bp paired-end libraries sequenced on the NovaSeq 6000 platform. The reference genes and genome annotation files were downloaded from the ENSEMBL website. The reference genome (GRCh38/hg38) was indexed using Bowtie v1.0.1, and the clean data were aligned to the reference genome using HISAT2 v2.1.0. FPKM (Fragments Per Kilobase Million Mapped Reads) values were calculated to estimate gene expression levels in each sample. Differentially expressed genes (DEGs) were identified using DESeq, with a fold change >2 and a P value <0.05 as the criteria. Gene Ontology and KEGG Pathway analyses were performed using Metascape. Original data were uploaded to the Sequence Read Archive (SRA) database (accession number: PRJNA1153572).

Statistical analysis

The results were statistically analyzed and graphed using SPSS 24.0 and GraphPad Prism 8.01 software. The calculated data conformed to normal distribution and are expressed as the mean ± standard deviation (mean±SD); those that did not conform to normal distribution were expressed as the median ± interquartile range (median±IQR). For comparisons between groups with a normal distribution and homogeneity of variance, analysis of variance (ANOVA) was used, and the least significant difference (LSD) test was used for pairwise comparisons. Otherwise, multiple independent sample rank sum tests were used, and a P value less than 0.05 was considered to indicate statistical significance.

RESULTS

Atelectasis in MPP: evolution and pulmonary fibrosis outcomes

Serial chest radiographs of a pediatric patient with a diagnosis of MPP were analyzed over 6 months to illustrate the progression from acute lung injury to fibrotic changes. The initial X-ray taken on January 30 revealed consolidation in the upper lobe of the right lung (Fig. 1A). Imaging performed on February 5 showed a reduction in the extent of consolidation, although atelectasis was evident (Fig. 1B). By February 20, the affected lung area demonstrated a persistent

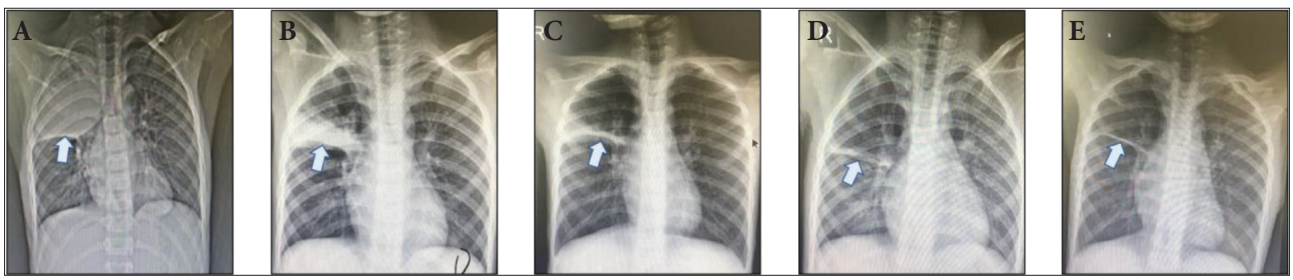

Fig. 1. Atelectasis in MPP. Evolution and pulmonary fibrosis outcomes. Serial chest radiographs of a pediatric patient with a diagnosis of MPP were analyzed over 6 months to illustrate the progression from acute lung injury to fibrotic changes. Taken on **A** – January 30, **B** – February 5, **C** – February 20, **D** – April 3, **E** – August 7.

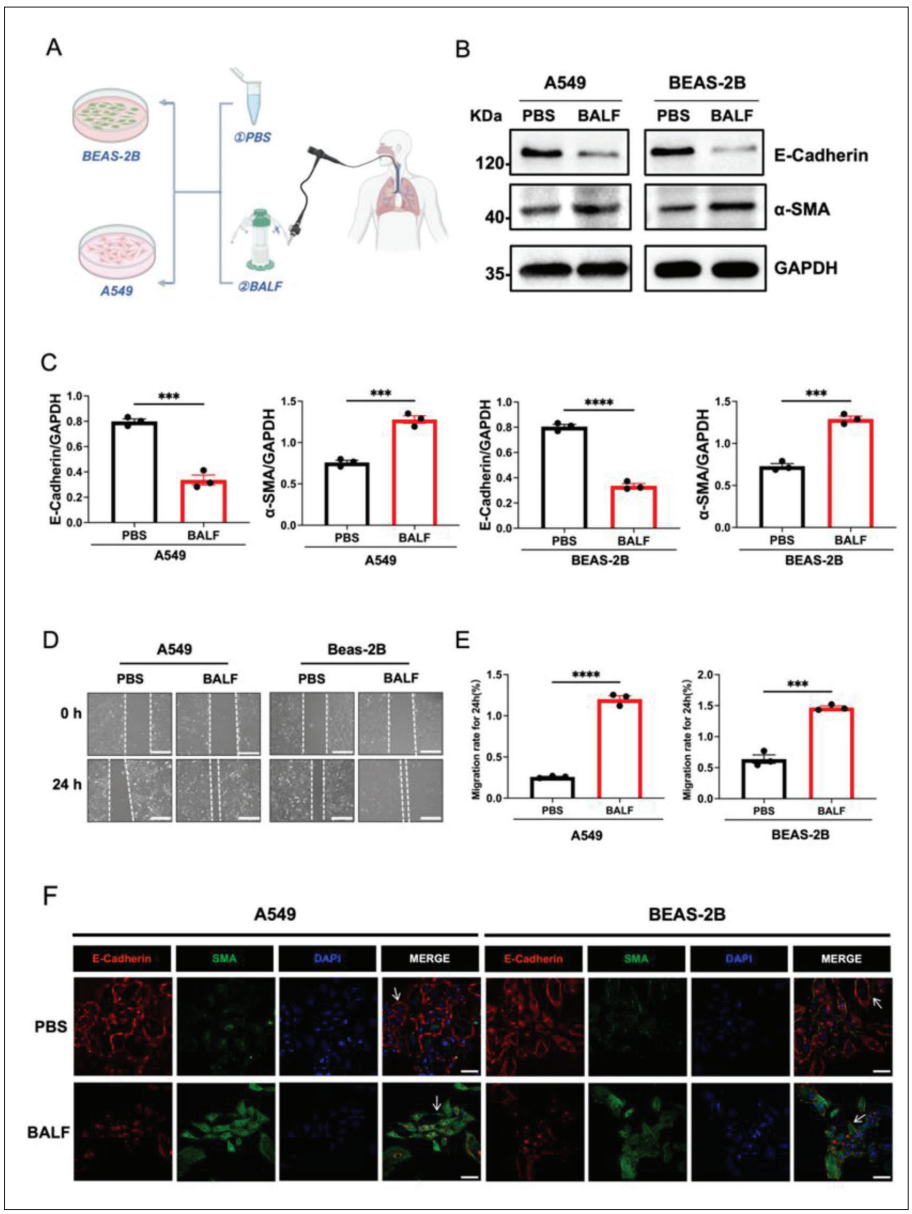

Fig. 2. The pulmonary microenvironment in MPP with atelectasis has the potential to induce EMT. **A** – Pattern map of BALF-treated cells. **B** – A549, **C** – BEAS-2B cells exposed to PBS or BALF for 72 h. The levels of α-SMA and E-cadherin in 2 cell lines were assessed by Western blotting. The values are the means±SD of 3 independent experiments. *P<0.05, **P<0.01, ***P<0.001. **D, E** – Scratch experiments and statistical migration values of cells after treatment in each group. Scale bars (white), 100 μm. *P<0.05, **P<0.01, ***P<0.001. **F** – Representative fluorescence photomicrographs showing the effect of each group on the expression of α-SMA (green), E-cadherin (red), DAPI (blue). Scale bars (white), 100 μm. Repeat experiments were performed to confirm the results with representative photographs shown. The arrows (white) indicate representative cell morphologies.

reduction in volume without any decrease in density (Fig. 1C). The consolidation continued to diminish over the following months, as can be observed in chest X-rays dated April 3 (Fig. 1D). By August 7, the high-density shadow in the upper right lobe was mostly resolved, leaving behind localized fibrotic changes (Fig. 1E). The sequential radiological results of this case demonstrate that patients with MPP complicated by atelectasis may ultimately develop long-term pulmonary fibrosis, and we speculate that this process is caused by EMT, a transformation that plays a critical role in the development of pulmonary fibrosis.

BALF from MPP patients with atelectasis has the potential to induce EMT

To investigate whether the pulmonary microenvironment in MPP patients with atelectasis can induce EMT, we treated A549 and BEAS-2B cells with BALF from patients diagnosed with MPP complicated by atelectasis (Fig. 2A) and then measured the levels of the intercellular adhesion protein E-cadherin and the interstitial marker α-SMA. The results showed that the expression of α-SMA was upregulated and that of E-cadherin was downregulated after BALF

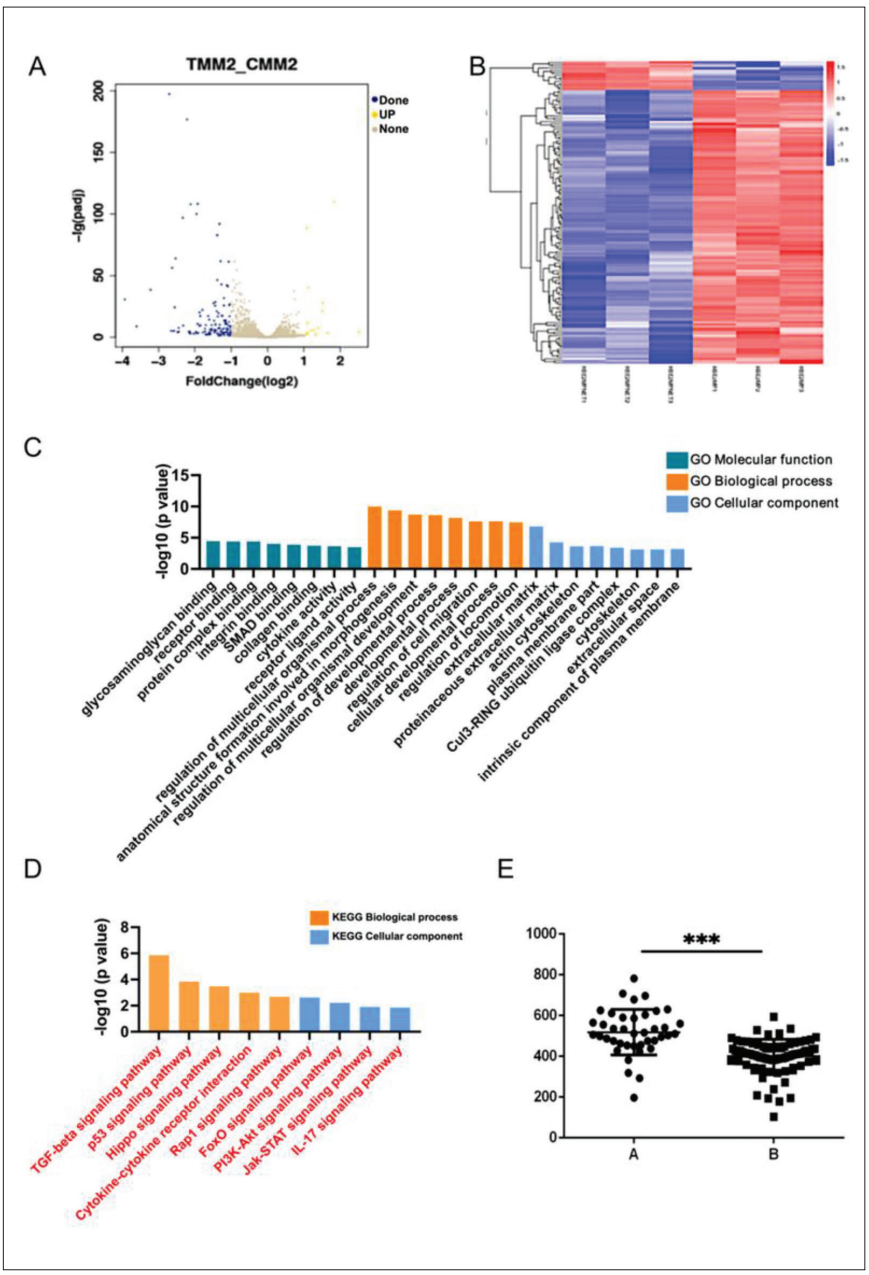

Fig. 3. RNA-seq showing that differentially expressed genes were most significantly enriched in the TGF-β signaling pathway. **A** – Volcano plot generated to visualize the DEGs between cells treated with BALF from MPP patients with atelectasis and the control group. The gene expression values are represented on a log2 scale. Upregulated genes are orange, downregulated genes are blue. **B** – Hierarchical clustering heatmap showing the RNA levels of these DEGs. The genes were ordered based on their fold change. **C** – GO enrichment analysis of differentially expressed genes involved in BALF intervention in alveolar epithelial cells. **D** – KEGG statistics expressed on a -log10 scale. **E** – 120 patients were divided into an atelectasis group A and a non-atelectasis group B, and TGF-β expression was measured using ELISA. The values are the means±SD of 3 independent experiments. *P<0.05, **P<0.01, ***P<0.001.

intervention compared to matching controls (P<0.05) (Fig. 2B and C). The scratches assay results revealed that after 24 h of intervention, the BALF treatment significantly promoted the migration of A549 and BEAS-2B cells (Fig. 2D and E). Immunofluorescence showed that after intervention with BALF from MPP patients with atelectasis, BEAS-2B and A549 cells tended to transition from their original cobblestone-like morphology to a spindle-like morphology, which is a typical phenotype of mesenchymal cells [21] (Fig. 2F). Additionally, the localization of the epithelial marker E-cadherin on the plasma membrane was disrupted and the formation of α-SMA was promoted (Fig. 2F), both of which are characteristic features of mesenchymal cells [21]. These findings provide evidence that the pulmonary microenvironment in MPP patients with atelectasis has the potential to induce EMT in bronchial epithelial cells.

Differentially expressed genes induced by BALF from MPP patients with atelectasis are significantly enriched in the TGF-β pathway

To investigate the signaling pathways involved in pulmonary microenvironment-mediated EMT, we analyzed the differences in RNA expression between pulmonary microenvironment-treated BEAS-2B cells and controls using RNA sequencing. A total of 158 DEGs (15 upregulated and 143 downregulated) were identified according to the criteria of fold change >2 and P<0.05 (Fig. 3A). Hierarchical clustering using heatmaps displayed the RNA levels of these DEGs, as well as genes associated with the pulmonary microenvironment-mediated EMT (Fig. 3B). Gene ontology (GO) enrichment analysis suggested that the DEGs were mainly enriched in biological

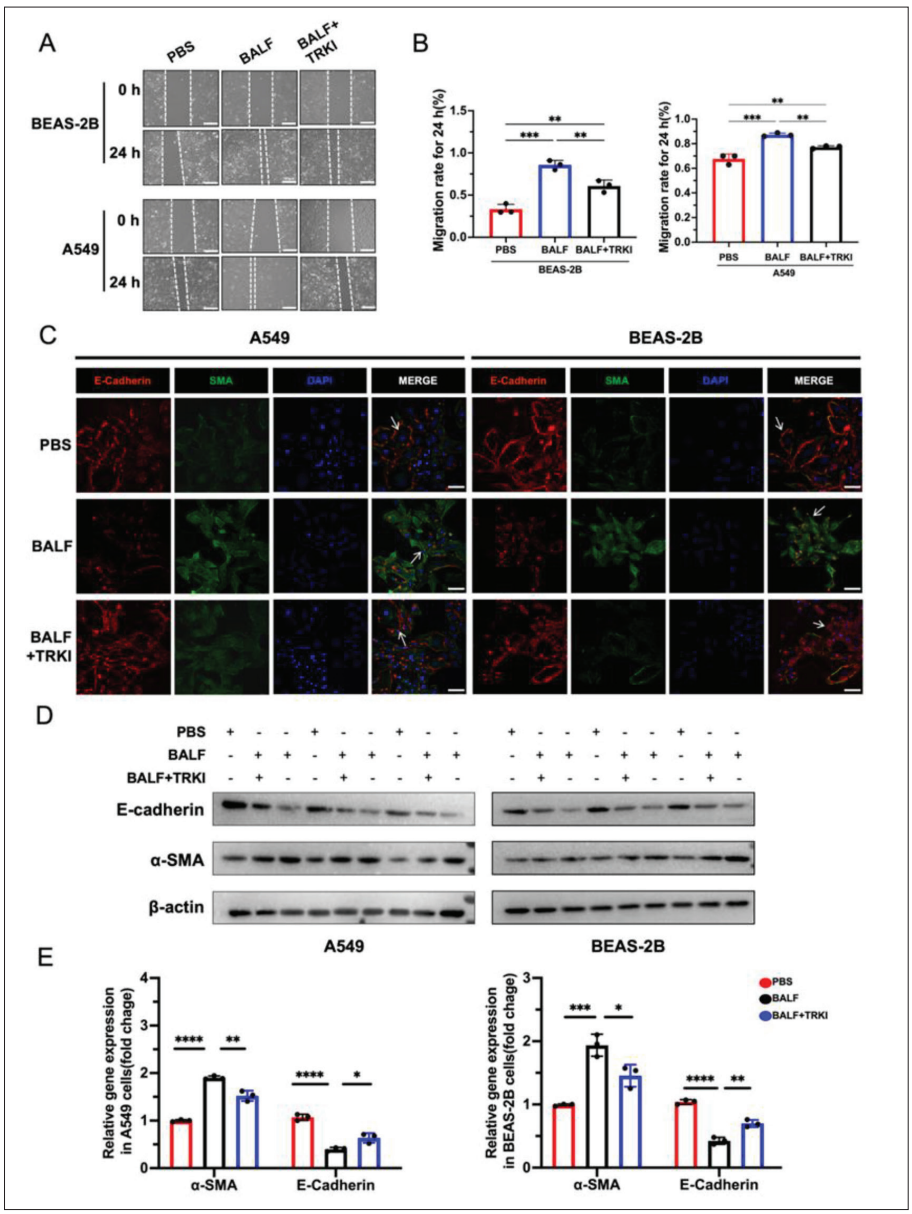

Fig. 4. TRKI can effectively reverse the EMT induced by BALF from MPP patients with atelectasis. **A, B** – Scratch experiments and statistical migration values of cells after treatment in each indicated group. Scale bars (white), 100 μm. The values are the means±SD of 3 independent experiments. *P<0.05, **P<0.01, ***P<0.001. **C** – Representative fluorescence photomicrographs showing the effect of each group on the expression of α-SMA (green), E-cadherin (red), DAPI (blue). Scale bars (white), 100 μm. Repeat experiments were performed to confirm the results; representative photographs are shown. The arrows (white) indicate representative cell morphologies. **D** – Western blotting experiments performed on cell lysates from each intervention group. **E** – The statistical values for the relative expression levels of α-SMA and E-cadherin in each group. The values are the means±SD of 3 independent experiments. *P<0.05, **P<0.01, ***P<0.001.

processes (Fig. 3C). KEGG pathway enrichment analysis revealed that signaling pathways such as the TGF-β, P53, Hippo, Rap1, FoxO, and PI3K-Akt and cytokine-cytokine receptor interaction pathways were significantly upregulated in BALF-treated cells, and that the DEGs were most prominently enriched in the TGF-β signaling pathway (Fig. 3D). To investigate this further, 120 MPP patients were divided into 2 groups, those with atelectasis and those without. Their sputum was diluted at a 1:1 ratio and the expression of TGF-β1 was measured using the ELISA. Our results revealed a statistically significant difference in TGF-β1 expression between the atelectasis and the non-atelectasis group (Fig. 3E).

Inhibiting the TGF-β pathway effectively mitigates EMT induced by BALF from MPP patients with atelectasis

The scratch assay results revealed that after 24 h of intervention, the BALF group significantly promoted the migration of BEAS-2B and A549 cells compared with the PBS group, and that the BALF + TRKI group showed a decrease in the migration rate compared with the BALF group (Fig. 4A and B). Therefore, in

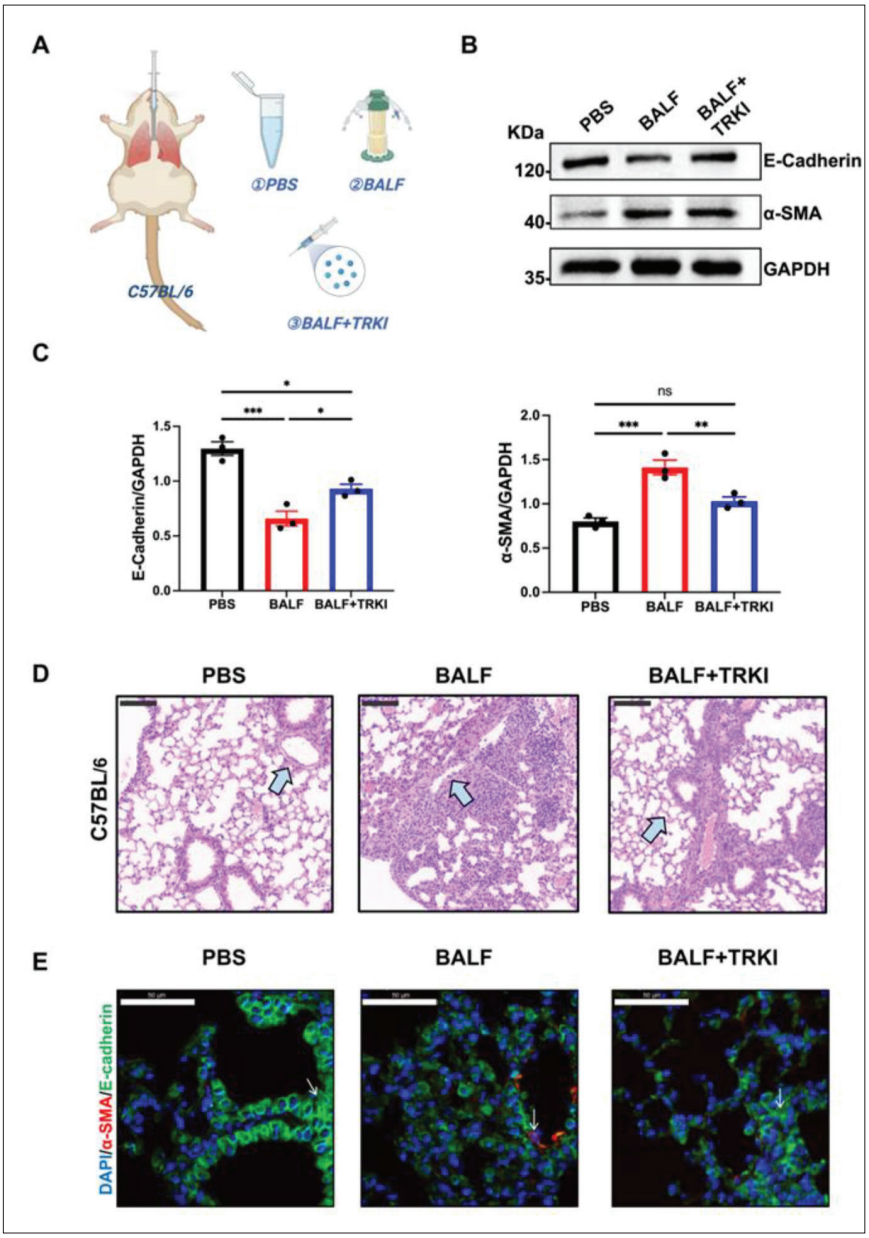

Fig. 5. TRKI exhibits significant inhibitory effects on inflammation and EMT in mouse lung tissue induced by BALF from MPP patients with atelectasis. **A** – Mice bronchially injected with PBS, BALF, BALF combined with TRKI for 3 days. **B** – Western blot experiments conducted using proteins extracted from the ground and lysed lung tissues of mice from the indicated groups. The levels of α-SMA and E-cadherin were measured by Western blotting as described. **C** – Statistical values of the expression levels of the target proteins in each group relative to the internal glyceraldehyde 3-phosphate dehydrogenase (GAPDH) control. The values are the means±SD of 3 independent experiments. *P<0.05, **P<0.01, ***P<0.001. **D** – Representative images of H&E-stained lung tissues. Scale bars (black), 100 μm. The arrows (white) indicate representative comparisons of lung injury or inflammatory infiltration. **E** – Representative fluorescence photomicrographs showing the effect of each group on the expression of α-SMA (red), E-cadherin (green), DAPI (blue). Scale bars (white), 100 μm. Repeat experiments were performed to confirm the results; representative photographs are shown. The arrows (white) indicate representative areas of the localization level of the target protein in the cells.

patients with MPP complicated by atelectasis, BALF significantly promoted the migration of lung tissue cells, while TRKI partially inhibited the migration of cells. Immunofluorescence results showed that inhibition of the TGF-β signaling pathway suppressed the formation of the spindle-like morphology in both cell lines (Fig. 4C). Additionally, inhibition of the TGF-β pathway significantly attenuated BALF-induced disruption of E-cadherin localization and the formation of α-SMA (Fig. 4C). Western blot analysis pointed to a significant downregulation in E-cadherin expression and upregulation of α-SMA in cells treated with BALF. These effects were reversed after treatment with BALF combined with the TRKI (Fig. 4D and E). The results suggest that inhibition of the TGF-β signaling pathway effectively mitigates the EMT induced by the pulmonary microenvironment in MPP with atelectasis.

TRKI exhibits significant inhibitory effects on inflammation and EMT in mouse lung tissue induced by BALF from MPP patients with atelectasis

Encouraged by the results above, we conducted experimental verification in mice. Mice were treated with PBS, BALF, or BALF combined with a TRKI for 3 days (Fig. 5A). Western blot analysis revealed that E-cadherin protein expression was significantly downregulated and α-SMA expression was significantly upregulated in lung tissues treated with BALF via intratracheal injection compared to the control group. Both changes were statistically significant. However, these alterations were reduced after the addition of TRKI compared to the group that received BALF alone (Fig. 5B and C), which aligns with the findings from the cell experiments. H&E staining of mouse lung tissue showed that the BALF

group exhibited extensive inflammatory cell infiltration and alveolar structural damage such as alveolar wall collapse, compared to the control group, with a significant increase in lung injury. The BALF + TRKI group also showed inflammatory cell infiltration and alveolar structural damage. Nonetheless, the level of inflammatory cell infiltration and the degree of damage were lower than in the BALF group (Fig. 5D). Immunofluorescence was used to assess the expression of E-cadherin and α-SMA in mouse lung tissue sections. Compared to the PBS group and the BALF + TRKI group, the BALF group showed a significant decrease in E-cadherin expression and a significant increase in α-SMA expression (Fig. 5E). These results suggest that the pulmonary microenvironment can induce EMT changes in mouse lung tissue through the TGF-β signaling pathway.

DISCUSSION

MP is considered a possible cause of lung infection in patients with pulmonary fibrosis [22]. There have been reports of chronic interstitial pulmonary fibrosis as a sequela of MPP [23, 24]. This is consistent with our observations from consecutive X-rays of an MPP patient. The finding that EMT is a key factor in the development of pulmonary fibrosis [20] prompted us to hypothesize that it may contribute to the progression of MPP with atelectasis into long-term pulmonary fibrosis.

Consequently, we conducted further *in vivo* and *in vitro* experiments and found that BALF from MPP patients with atelectasis significantly increased the migratory ability of BEAS-2B and A549 cells, and induced the reduction of the epithelial marker E-cadherin and the formation of α-SMA in both cell lines and mouse lung tissue, which are typical features of EMT [21]. Moreover, both cell lines exhibited a tendency to shift from their original cobblestone-like morphology to a spindle-shaped appearance, providing further evidence of the cells' mesenchymal transformation [21]. These changes suggest that BALF from MPP patients with atelectasis has the potential to induce EMT in the lungs.

Our transcriptome sequencing analysis showed that after treatment with BALF from MPP patients with atelectasis, several pathways – including TGF-β, P53, Hippo signaling, cytokine-cytokine receptor interaction, Rap1, FoxO, and the phosphatidylinositol 3-kinase and protein kinase B (PI3K-Akt) pathways – were significantly upregulated. Among these, the differentially expressed genes were most notably enriched in the TGF-β signaling pathway. Previous studies have shown that the TGF-β and PI3K-Akt signaling pathways are closely related to EMT [25, 26]. Additionally, Satoshi et al. [21] indicated that the Rap1, FoxO, and P53 signaling pathways, and cytokine-cytokine receptor interaction were significantly upregulated in EMT-associated lncRNA induced by TGFβ1 (ELIT-1)-induced EMT phenomena [21], which is consistent with our sequencing results.

Notably, the inhibition of the TGF-β pathway suppressed the formation of spindle-like morphology in both cell lines and significantly reduced the BALF-induced disruption of E-cadherin localization and the formation of α-SMA. This highlights the critical role of the TGF-β signaling pathway in this pathological process and suggests a potential link to the development of pulmonary fibrosis. Sgalla et al. [27] reported that the mRNA and protein levels of TGF-β were upregulated in lung endothelial cells isolated from a bleomycin-induced fibrosis model, which is consistent with our experimental results.

As a crucial component of the pulmonary microenvironment, BALF plays a significant role in the evaluation of lung diseases, confirming or ruling out infections, identifying cancer cells, and assessing and diagnosing interstitial lung diseases [27-29]. Therefore, we used BALF from MPP patients with atelectasis as representative of their pulmonary microenvironment's ability to intervene in both cell and mouse models. Due to the relatively low proportion of MPP patients undergoing bronchoscopy and the limited time available for sample collection, sputum samples were used for ELISA detection. This choice was informed by existing literature indicating that sputum analysis is a less invasive tool than BALF and is suitable for predicting and monitoring lung inflammation [30]. Moreover, sputum can yield reliable measurements of TGF-β levels in patients [30]. Therefore, we opted for sputum samples to ensure statistical significance in the ELISA while obtaining reliable TGF-β data.

Alveolar epithelial cells (AECs), as highly plastic "multipotent" progenitor cells, have the potential to

regenerate normal alveolar structures through re-epithelialization or to transdifferentiate into fibroblasts via EMT [31, 32]. It has been reported that cell lines derived from type II AECs frequently undergo EMT, and the excessive proliferation and hypertrophy of type II AECs are involved in the regulation of pulmonary fibrosis [33, 34]. A549 cells, as adenocarcinoma alveolar basal epithelial cells, have become an ideal model for studying type II alveolar epithelial cells [35]. Additionally, A549 cells naturally express epithelial markers and can easily induce EMT under stimuli such as TGF-β, hypoxia, or inflammatory cytokines, with the associated molecular pathways of EMT well characterized, making them suitable models for studying EMT mechanisms in the context of pneumonia [11, 36, 37]. BEAS-2B, a human bronchial epithelial cell line closely related to type II human AECs, also undergoes EMT and contributes to the pathology of pulmonary fibrosis under certain conditions [38]. Therefore, we chose BEAS-2B and A549 cell lines to study the relationship between EMT and BALF.

E-cadherin and α-SMA were selected as EMT markers based on practices and research from literature. EMT is triggered by a series of molecular events, such as the suppression of E-cadherin expression, the induction of vimentin, and the loss of cell-cell junctions [39]. These events are typically accompanied by other signals involved in cytoskeletal remodeling, such as the formation of actin stress fibers and the induction of α-SMA. Loss of E-cadherin is one of the primary markers of EMT [11]. Moreover, myofibroblasts are considered to play a crucial role in the pathogenesis of pulmonary fibrosis [40]. Myofibroblasts produce large amounts of matrix proteins and express contractile proteins such as α-SMA, regarded as the most reliable marker of the myofibroblast phenotype [41-43].

TGF-β, as a potent inducer of EMT, has a key role in the pathogenesis of diseases such as idiopathic pulmonary fibrosis (IPF) and lung cancer. Artur et al. [45] demonstrated that TGF-β levels in BALF positively correlate with high-resolution computed tomography (HRCT) scores, suggesting that TGF-β is a good marker for fibrosis in diffuse parenchymal lung disease (DPLD). The positive correlation between TGF-β levels and fibrosis markers further supports this, indicating that TGF-β is a reliable biomarker for assessing the severity of fibrosis-related lung diseases. Moreover, EMT has been widely recognized as essential for cancer cells to acquire invasive and metastatic phenotypes [44]. The loss of apical-basal polarity in epithelial cells and the acquisition of mesenchymal traits, which coordinate the biological mechanisms that enhance their migratory and invasive capabilities, are crucial for tumor metastasis [45, 46]. TGF-β plays a central role in driving EMT in lung cancer by downregulating E-cadherin and upregulating mesenchymal markers such as vimentin and α-SMA, making it a potent inducer of EMT. This is consistent with our findings in MPP patients. TGF-β inhibits cell proliferation in the early stages of lung cancer; however, in later stages, TGF-β promotes tumor progression and metastasis through the induction of EMT. This dual role underscores its importance in the pathogenesis of the disease [47, 48]. This pathway involves typical Smad-dependent signaling, where transcription factors such as SMAD2, SMAD3, and SMAD4 mediate the effects of TGF-β on EMT [49]. Additionally, the ability of TGF-β to induce EMT is associated with the development of stem-like characteristics in cancer cells, which contributes to the observed invasiveness and treatment resistance in lung cancer [49]. Connecting the mechanisms of TGF-β-induced cancer-related EMT provides new insights for further investigations into the molecular mechanisms underlying EMT in MPP patients.

Gao et al. [52] conducted transcriptome sequencing on the BALF of children with MPP, revealing a significant upregulation of natural killer cell-mediated cytotoxicity and T cell receptor signaling pathways. TGF-β is secreted by immune cells such as T lymphocytes through autocrine or paracrine mechanisms [50, 51]. Upregulation of the T cell receptor signaling pathway leads to increased secretion of TGF-β, which in turn promotes proliferation and fibrosis. We hypothesize that this mechanism may be a potential factor in the pulmonary microenvironment of MPP patients with atelectasis, driving the induction of EMT. Additionally, Satoshi et al. propose that the TGF-β/Smad-ELIT-1 axis functions as a complex system for amplifying and sustaining TGF-β signaling [52]. When the TGF-β receptor is activated, ELIT-1 binds to Smad3, promoting EMT progression through TGF-β/Smad3 signaling. This suggests that this pathway may also be a potential mechanism by which BALF induces EMT in our study, though further research is needed to confirm this.

Additionally, it was demonstrated that the C-terminal residues of MP P1 adhesin (P1-C) can induce ECM deposition and EMT in the lungs following MP infection [20]. Therefore, the occurrence of EMT in the lungs of MPP patients may not influenced only be by the pulmonary microenvironment, as investigated in our study, but also by the direct effects of MP. This suggests that the direct involvement of MP components is another critical factor contributing to the progression of MPP in patients to pulmonary fibrosis. Future research could further explore the mechanisms of pulmonary fibrosis in MPP patients by examining the interaction between MP and the pulmonary microenvironment.

This study has several limitations. First, the experimental design included only a limited number of EMT markers. Future research should expand the analysis to include a wider range of markers and typical phenotypes, utilizing scanning electron microscopy (SEM) for more detailed observation of cell morphological changes, along with ECM detection for a more comprehensive assessment of EMT. Second, when examining BALF samples from MPP patients, we observed that inflammatory cells and detached epithelial cells predominated. Our study concentrated on the effects of overall changes in the pulmonary microenvironment on lung epithelial cells. Therefore, we did not further classify or quantify these cells. However, future studies could benefit from a more detailed analysis of BALF cell composition, which could provide additional mechanistic insights. Additionally, the sample size in our study was relatively small. Future research should include larger, multicenter cohorts to increase the generalizability of the results. Finally, this study relied solely on chemical inhibitors. Future research could incorporate gene knockout or overexpression techniques to explore other pathways interacting with TGF-β signaling to elucidate more specific mechanisms leading to pulmonary fibrosis in MPP patients with atelectasis.

CONCLUSIONS

This study suggests that the pulmonary microenvironment in MPP patients with atelectasis contributes to the induction of EMT in the lungs, with the TGF-β signaling pathway playing a pivotal role in this process. This may represent a key mechanism underlying the development of pulmonary fibrosis in MPP patients with atelectasis. These findings highlight the importance of focusing on the pulmonary microenvironment in MPP patients and exploring TGF-β pathway-targeted therapeutic strategies for the clinical prevention and management of pulmonary fibrosis. Further research is essential to investigate the underlying mechanisms and explore other pathways involved in the development of pulmonary fibrosis in MPP patients, ultimately leading to the development of more effective treatments.

Funding: This work was supported by grants from the Wuxi Taihu Lake Talent Plan (Grant No. DJTD202304), the Natural Science Foundation of Jiangsu Province (Grants No. BK20230189), Wuxi Municipal Bureau on Science and Technology (Grant No. K20221033), the Top Talent Support Program for young and middle-aged researchers of Wuxi Health Committee (Grant No. BJ2023089).

Acknowledgments: We thank Jiangsu Organ Transplantation Research Institute and Wuxi People's Hospital for providing the research platform.

Author contributions: Lu Fan and Huixia Wang contributed equally to the work. Conceptualization – Yun Guo, and Ling Li; writing, original draft preparation, validation, formal analysis – Lu Fan; investigation, software – Huixia Wang; resources – Nuo Xu; data curation, methodology, writing, review and editing – Yun Guo; visualization, supervision, project administration, funding acquisition – Ling Li. All authors have read and agreed to the published version of the manuscript.

Conflict of interest disclosure: The authors declare no conflicts of interest.

Data availability: Data underlying the reported findings have been provided as a raw dataset, which is available here: https://www.serbiosoc.org.rs/NewUploads/Uploads/Fan%20et%20al_Dataset.xls

REFERENCES

1. Beeton ML, Zhang XS, Uldum SA, Bebear C, Dumke R, Gullsby K, Ieven M, Loens K, Nir-Paz R, Pereyre S, Spiller OB, Chalker VJ, Mycoplasma ESGf, Chlamydia Infections Mycoplasma pneumoniae s, Mycoplasma ESGf, Chlamydia Infections Mycoplasma pneumoniae subgroup members not listed as an individual a. Mycoplasma pneumoniae infections, 11 countries in Europe and Israel, 2011 to 2016. Euro Surveill. 2020;25(2). https://doi.org/10.2807/1560-7917.ES.2020.25.2.1900112
2. Guo DX, Hu WJ, Wei R, Wang H, Xu BP, Zhou W, Ma SJ, Huang H, Qin XG, Jiang Y, Dong XP, Fu XY, Shi DW, Wang LY, Shen AD, Xin DL. Epidemiology and mechanism of drug resistance of Mycoplasma pneumoniae in Beijing, China: A multicenter study. Bosn J Basic Med Sci. 2019;19(3):288-96. https://doi.org/10.17305/bjbms.2019.4053

3. Go JR, Ali NS, Berbari EF. Mycoplasma pneumoniae-Induced Rash and Mucositis. Mayo Clin Proc. 2021;96(6):1520-1. https://doi.org/10.1016/j.mayocp.2021.03.009
4. Chen S, Ding Y, Vinturache A, Gu H, Lu M, Ding G. Pulmonary embolism associated with mycoplasma in a child. Lancet Infect Dis. 2020;20(11):1347. https://doi.org/10.1016/S1473-3099(20)30253-X
5. Song WJ, Kang B, Lee HP, Cho J, Lee HJ, Choe YH. Pediatric Mycoplasma pneumoniae Infection Presenting with Acute Cholestatic Hepatitis and Other Extrapulmonary Manifestations in the Absence of Pneumonia. Pediatr Gastroenterol Hepatol Nutr. 2017;20(2):124-9. https://doi.org/10.5223/pghn.2017.20.2.124
6. 6. Hubert D, Dumke R, Weichert S, Welker S, Tenenbaum T, Schroten H. Emergence of Macrolide-Resistant Mycoplasma pneumoniae during an Outbreak in a Primary School: Clinical Characterization of Hospitalized Children. Pathogens. 2021;10(3). https://doi.org/10.3390/pathogens10030328
7. Wang X, Zhong LJ, Chen ZM, Zhou YL, Ye B, Zhang YY. Necrotizing pneumonia caused by refractory Mycoplasma pneumonia pneumonia in children. World J Pediatr. 2018;14(4):344-9. https://doi.org/10.1007/s12519-018-0162-6
8. Xu Q, Zhang L, Hao C, Jiang W, Tao H, Sun H, Huang L, Zhou J, Fan L. Prediction of Bronchial Mucus Plugs Formation in Patients with Refractory Mycoplasma Pneumoniae Pneumonia. J Trop Pediatr. 2017;63(2):148-54. https://doi.org/10.1093/tropej/fmw064
9. Piccione J, Hysinger EB, Vicencio AG. Pediatric advanced diagnostic and interventional bronchoscopy. Semin Pediatr Surg. 2021;30(3):151065. https://doi.org/10.1016/j.sempedsurg.2021.151065
10. Su DQ, Li JF, Zhuo ZQ. Clinical Analysis of 122 Cases with Mycoplasma Pneumonia Complicated with Atelectasis: A Retrospective Study. Adv Ther. 2020;37(1):265-71. https://doi.org/10.1007/s12325-019-01129-8
11. Kalluri R, Weinberg RA. The basics of epithelial-mesenchymal transition. J Clin Invest. 2009;119(6):1420-8. https://doi.org/10.1172/JCI39104
12. Rock JR, Barkauskas CE, Cronce MJ, Xue Y, Harris JR, Liang J, Noble PW, Hogan BL. Multiple stromal populations contribute to pulmonary fibrosis without evidence for epithelial to mesenchymal transition. Proc Natl Acad Sci U S A. 2011;108(52):E1475-83. https://doi.org/10.1073/pnas.1117988108
13. Lee HW, Jose CC, Cuddapah S. Epithelial-mesenchymal transition: Insights into nickel-induced lung diseases. Semin Cancer Biol. 2021;76:99-109. https://doi.org/10.1016/j.semcancer.2021.05.020
14. Garcia-Cuellar CM, Santibanez-Andrade M, Chirino YI, Quintana-Belmares R, Morales-Barcenas R, Quezada-Maldonado EM, Sanchez-Perez Y. Particulate Matter (PM(10)) Promotes Cell Invasion through Epithelial-Mesenchymal Transition (EMT) by TGF-beta Activation in A549 Lung Cells. Int J Mol Sci. 2021;22(23). https://doi.org/10.3390/ijms222312632
15. Nieto MA, Huang RY, Jackson RA, Thiery JP. EMT: 2016. Cell. 2016;166(1):21-45. https://doi.org/10.1016/j.cell.2016.06.028
16. Vizarraga D, Kawamoto A, Matsumoto U, Illanes R, Perez-Luque R, Martin J, Mazzolini R, Bierge P, Pich OQ, Espasa M, Sanfeliu I, Esperalba J, Fernandez-Huerta M, Scheffer MP, Pinyol J, Frangakis AS, Lluch-Senar M, Mori S, Shibayama K, Kenri T, Kato T, Namba K, Fita I, Miyata M, Aparicio D. Immunodominant proteins P1 and P40/P90 from human pathogen Mycoplasma pneumoniae. Nat Commun. 2020;11(1):5188. https://doi.org/10.1038/s41467-020-18777-y
17. Grosshennig S, Ischebeck T, Gibhardt J, Busse J, Feussner I, Stulke J. Hydrogen sulfide is a novel potential virulence factor of Mycoplasma pneumoniae: characterization of the unusual cysteine desulfurase/desulfhydrase HapE. Mol Microbiol. 2016;100(1):42-54. https://doi.org/10.1111/mmi.13300
18. Becker A, Kannan TR, Taylor AB, Pakhomova ON, Zhang Y, Somarajan SR, Galaleldeen A, Holloway SP, Baseman JB, Hart PJ. Structure of CARDS toxin, a unique ADP-ribosylating and vacuolating cytotoxin from Mycoplasma pneumoniae. Proc Natl Acad Sci U S A. 2015;112(16):5165-70. https://doi.org/10.1073/pnas.1420308112
19. Zheng S, Wang Q, D'Souza V, Bartis D, Dancer R, Parekh D, Gao F, Lian Q, Jin S, Thickett DR. ResolvinD(1) stimulates epithelial wound repair and inhibits TGF-beta-induced EMT whilst reducing fibroproliferation and collagen production. Lab Invest. 2018;98(1):130-40. https://doi.org/10.1038/labinvest.2017.114
20. Shi J, Ma C, Hao X, Luo H, Li M. Reserve of Wnt/β-catenin Signaling Alleviates Mycoplasma pneumoniae P1-C-induced Inflammation in airway epithelial cells and lungs of mice. Mol Immunol. 2023;153:60-74. https://doi.org/10.1016/j.molimm.2022.11.003
21. Sakai S, Ohhata T, Kitagawa K, Uchida C, Aoshima T, Niida H, Suzuki T, Inoue Y, Miyazawa K, Kitagawa M. Long Noncoding RNA ELIT-1 Acts as a Smad3 Cofactor to Facilitate TGFβ/Smad Signaling and Promote Epithelial-Mesenchymal Transition. Cancer Res. 2019;79(11):2821-38. https://doi.org/10.1158/0008-5472.Can-18-3210
22. Pittet LF, Bertelli C, Scherz V, Rochat I, Mardegan C, Brouillet R, Jaton K, Mornand A, Kaiser L, Posfay-Barbe K, Asner SA, Greub G. Chlamydia pneumoniae and Mycoplasma pneumoniae in children with cystic fibrosis: impact on bacterial respiratory microbiota diversity. Pathog Dis. 2021;79(1). https://doi.org/10.1093/femspd/ftaa074
23. Tablan OC, Reyes MP. Chronic interstitial pulmonary fibrosis following Mycoplasma pneumoniae pneumonia. Am J Med. 1985;79(2):268-70. https://doi.org/10.1016/0002-9343(85)90021-x
24. Lin Y, Tan D, Kan Q, Xiao Z, Jiang Z. The Protective Effect of Naringenin on Airway Remodeling after Mycoplasma Pneumoniae Infection by Inhibiting Autophagy-Mediated Lung Inflammation and Fibrosis. Mediators Inflamm. 2018;2018:8753894. https://doi.org/10.1155/2018/8753894
25. Gazzillo A, Polidoro MA, Soldani C, Franceschini B, Lleo A, Donadon M. Relationship between Epithelial-to-Mesenchymal Transition and Tumor-Associated Macrophages in Colorectal Liver Metastases. Int J Mol Sci. 2022;23(24). https://doi.org/10.3390/ijms232416197

26. Ma Z, Lou S, Jiang Z. PHLDA2 regulates EMT and autophagy in colorectal cancer via the PI3K/AKT signaling pathway. Aging (Albany NY). 2020;12(9):7985-8000. https://doi.org/10.18632/aging.103117
27. Hogea SP, Tudorache E, Pescaru C, Marc M, Oancea C. Bronchoalveolar lavage: role in the evaluation of pulmonary interstitial disease. Expert Rev Respir Med. 2020;14(11):1117-30. https://doi.org/10.1080/17476348.2020.1806063
28. Meyer KC. Bronchoalveolar lavage as a diagnostic tool. Semin Respir Crit Care Med. 2007;28(5):546-60. https://doi.org/10.1055/s-2007-991527
29. Efared B, Ebang-Atsame G, Rabiou S, Diarra AS, Tahiri L, Hammas N, Smahi M, Amara B, Benjelloun MC, Serraj M, Chbani L, El Fatemi H. The diagnostic value of the bronchoalveolar lavage in interstitial lung diseases. J Negat Results Biomed. 2017;16(1):4. https://doi.org/10.1186/s12952-017-0069-0
30. Jing Y, Chen L, Geng L, Shan Z, Yang J. The levels of vitamins and cytokines in serum of elderly patients with community-acquired pneumonia: A case-control study. Health Sci Rep. 2023;6(12):e1737. https://doi.org/10.1002/hsr2.1737
31. Harada T, Nabeshima K, Hamasaki M, Uesugi N, Watanabe K, Iwasaki H. Epithelial-mesenchymal transition in human lungs with usual interstitial pneumonia: quantitative immunohistochemistry. Pathol Int. 2010;60(1):14-21. https://doi.org/10.1111/j.1440-1827.2009.02469.x
32. Kim KK, Kugler MC, Wolters PJ, Robillard L, Galvez MG, Brumwell AN, Sheppard D, Chapman HA. Alveolar epithelial cell mesenchymal transition develops in vivo during pulmonary fibrosis and is regulated by the extracellular matrix. Proc Natl Acad Sci U S A. 2006;103(35):13180-5. https://doi.org/10.1073/pnas.0605669103
33. Tan WJ, Tan QY, Wang T, Lian M, Zhang L, Cheng ZS. Calpain 1 regulates TGF-β1-induced epithelial-mesenchymal transition in human lung epithelial cells via PI3K/Akt signaling pathway. Am J Transl Res. 2017;9(3):1402-9.
34. Königshoff M, Kramer M, Balsara N, Wilhelm J, Amarie OV, Jahn A, Rose F, Fink L, Seeger W, Schaefer L, Günther A, Eickelberg O. WNT1-inducible signaling protein-1 mediates pulmonary fibrosis in mice and is upregulated in humans with idiopathic pulmonary fibrosis. J Clin Invest. 2009;119(4):772-87. https://doi.org/10.1172/jci33950
35. Foster KA, Oster CG, Mayer MM, Avery ML, Audus KL. Characterization of the A549 cell line as a type II pulmonary epithelial cell model for drug metabolism. Exp Cell Res. 1998;243(2):359-66. https://doi.org/10.1006/excr.1998.4172
36. Giard DJ, Aaronson SA, Todaro GJ, Arnstein P, Kersey JH, Dosik H, Parks WP. In vitro cultivation of human tumors: establishment of cell lines derived from a series of solid tumors. J Natl Cancer Inst. 1973;51(5):1417-23. https://doi.org/10.1093/jnci/51.5.1417
37. Thiery JP. Epithelial-mesenchymal transitions in tumour progression. Nat Rev Cancer. 2002;2(6):442-54. https://doi.org/10.1038/nrc822
38. Zoz DF, Lawson WE, Blackwell TS. Idiopathic pulmonary fibrosis: a disorder of epithelial cell dysfunction. Am J Med Sci. 2011;341(6):435-8. https://doi.org/10.1097/MAJ.0b013e31821a9d8e
39. Kourtidis A, Lu R, Pence LJ, Anastasiadis PZ. A central role for cadherin signaling in cancer. Exp Cell Res. 2017;358(1):78-85. https://doi.org/10.1016/j.yexcr.2017.04.006
40. Hinz B, Phan SH, Thannickal VJ, Galli A, Bochaton-Piallat ML, Gabbiani G. The myofibroblast: one function, multiple origins. Am J Pathol. 2007;170(6):1807-16. https://doi.org/10.2353/ajpath.2007.070112
41. Biernacka A, Dobaczewski M, Frangogiannis NG. TGF-β signaling in fibrosis. Growth Factors. 2011;29(5):196-202. https://doi.org/10.3109/08977194.2011.595714
42. Tomasek JJ, Gabbiani G, Hinz B, Chaponnier C, Brown RA. Myofibroblasts and mechano-regulation of connective tissue remodelling. Nat Rev Mol Cell Biol. 2002;3(5):349-63. https://doi.org/10.1038/nrm809
43. Desmoulière A, Chaponnier C, Gabbiani G. Tissue repair, contraction, and the myofibroblast. Wound Repair Regen. 2005;13(1):7-12. https://doi.org/10.1111/j.1067-1927.2005.130102.x
44. Brabletz T, Kalluri R, Nieto MA, Weinberg RA. EMT in cancer. Nat Rev Cancer. 2018;18(2):128-34. https://doi.org/10.1038/nrc.2017.118
45. García-Cuellar CM, Santibáñez-Andrade M, Chirino YI, Quintana-Belmares R, Morales-Bárcenas R, Quezada-Maldonado EM, Sánchez-Pérez Y. Particulate Matter (PM(10)) Promotes Cell Invasion through Epithelial-Mesenchymal Transition (EMT) by TGF-β Activation in A549 Lung Cells. Int J Mol Sci. 2021;22(23). https://doi.org/10.3390/ijms222312632
46. Chaffer CL, San Juan BP, Lim E, Weinberg RA. EMT, cell plasticity and metastasis. Cancer Metastasis Rev. 2016;35(4):645-54. https://doi.org/10.1007/s10555-016-9648-7
47. Wang X, Eichhorn PJA, Thiery JP. TGF-β, EMT, and resistance to anti-cancer treatment. Semin Cancer Biol. 2023;97:1-11. https://doi.org/10.1016/j.semcancer.2023.10.004
48. Liu LC, Tsao TC, Hsu SR, Wang HC, Tsai TC, Kao JY, Way TD. EGCG inhibits transforming growth factor-β-mediated epithelial-to-mesenchymal transition via the inhibition of Smad2 and Erk1/2 signaling pathways in nonsmall cell lung cancer cells. J Agric Food Chem. 2012;60(39):9863-73. https://doi.org/10.1021/jf303690x
49. Hwang JS, Lai TH, Ahmed M, Pham TM, Elashkar O, Bahar E, Kim DR. Regulation of TGF-β1-Induced EMT by Autophagy-Dependent Energy Metabolism in Cancer Cells. Cancers (Basel). 2022;14(19). https://doi.org/10.3390/cancers14194845
50. Gao M, Wang K, Yang M, Meng F, Lu R, Zhuang H, Cheng G, Wang X. Transcriptome Analysis of Bronchoalveolar Lavage Fluid From Children With Mycoplasma pneumoniae Pneumonia Reveals Natural Killer and T Cell-Proliferation Responses. Front Immunol. 2018;9:1403. https://doi.org/10.3389/fimmu.2018.01403
51. Moustakas A, Pardali K, Gaal A, Heldin CH. Mechanisms of TGF-beta signaling in regulation of cell growth and differentiation. Immunol Lett. 2002;82(1-2):85-91. https://doi.org/10.1016/s0165-2478(02)00023-8
52. Miyazono K, Katsuno Y, Koinuma D, Ehata S, Morikawa M. Intracellular and extracellular TGF-β signaling in cancer: some recent topics. Front Med. 2018;12(4):387-411. https://doi.org/10.1007/s11684-018-0646-8

SUPPLEMENTARY MATERIAL

Supplementary Table S1. Characteristics, clinical symptoms, and laboratory tests of MPP patients based on whether diagnosed with atelectasis. Data are presented as the mean±SD, median±interquartile range (IQR) or n (%), unless otherwise specified. P values<0.05 were considered statistically significant. CRP: C-reactive protein; WBC: white blood cells; HB: hemoglobin; PLT: platelet; ALT: alanine aminotransferase; AST: aspartate aminotransferase; LDH: lactate dehydrogenase; CK: creatine kinase. Normally distributed data are expressed as the mean±SD, non-normally distributed data are expressed as the median±IQR.

Characteristics	MPP with atelectasis (n=60)	MPP without atelectasis (n=60)	P Values
Age (year, mean±SD)	6.51±2.75	5.70±3.01	0.126
Female, n (%)	25(41.67)	28(46.67)	0.581
Cough, n (%)	60(100)	60(100)	/
Fever, n (%)	54(90)	55(91.67)	0.752
Fever days, mean±SD	5.63±4.23	5.39±2.96	0.091
Pleural effusion, n (%)	41(68.33)	20(33.33)	<0.001
CRP (mg/L), mean±SD	22.23±41.56	13.34±13.24	0.1172
WBC (10^9/L), mean±SD	8.86±4.77	8.57±5.09	0.748
Neutrophil percentage (%), mean±SD	61.41±11.80	59.43±13.02	0.385
Neutrophil counts(10^9/L), mean±SD	5.65±3.96	5.35±4.56	0.698
HB(g/L), mean±SD	128.43±11.36	129.63±12.43	0.582
PLT (10^9/L), mean±SD	234.78±84.83	262.93±101.43	0.102
ALT (U/L), mean±SD	20.43±23.87	15.24±6.76	0.108
AST (U/L), mean±SD	38.83±18.20	36.77±10.48	0.448
LDH (U/L), mean±SD	387.10±190.98	371.60±123.81	0.599
CK (U/L), mean±SD	95.65±88.11	94.12±50.17	0.907
CK-MB (U/L), mean±SD	14.37±8.41	15.74±9.74	0.412
Glucocorticoid application, n (%)	50(83.33%)	30(50.0)	<0.001
Hospitalization days, mean±SD	8.51±1.87	7.14±1.96	<0.001
Bronchoalveolar lavage, n (%)	35(58.33)	3(5)	<0.001
Sputum, n (%)	60(100)	60(100)	/